

## STUDY OF METHODS FOR THE SEISMIC DESIGN OF A MACHINE FOR PAPER PRODUCTION

**Rodrigo S. Morcelli, Reyolando M.L.R.F. Brasil**

*Departamento de Engenharia de Estruturas, Escola Politécnica, Universidade de São Paulo, São Paulo, Brazil*

**Keywords:** seismic analysis, seismic design, paper machine.

**Abstract.** The progresses in codes and the technical literature regarding seismic analyses emphasize, commonly, civil buildings and their dynamic behavior. Nevertheless, periodically, the dimensioning and construction of equipments or structures with distinct geometry and behavior are required. In numerous codes, though, statements that the comprised information is to be fully applied exclusively to seismic resistant configurations similar to the ones from typical buildings are found.

In these codes, issued by many countries for the construction in their respective territory, there are procedures and criteria established for the seismic design. Moreover, applicable analysis methods are presented, and the selection of which one to employ is based on details as type of resisting frame, intended occupation, rebuilding costs, significance and the geological features of the erection site.

In this paper, the study of part of a machine for paper production, regarding seismic analysis and by means of the Finite Element Method is presented. This machine consists of, essentially, a metallic frame supporting rotors, whose surfaces are in contact with the paper web. The methods usually found in codes, equivalent lateral force, spectrum analysis and analysis with acceleration time history were used, and their results compared and commented afterwards.

A better understanding of the methods and input parameters appropriate for the structure in study was intended, as well as of any eventual deviation caused by their selection. Special emphasis was applied to requirements found in the Brazilian code for seismic design.

## 1 INTRODUCTION

Typically, standards and directives for seismic resistant design focus on civil buildings, or structures with similar construction and dynamic behavior. The protection of human lives and structural damage control are the most important seismic performance requirements, in order to avoid collapse and in some cases allow prompt reoccupation. These documents are generally emitted by official entities or committees for application in their respective territory, and institute, among other subjects, proceedings and criteria for dimensioning and resistant configurations recommended or prohibited. Important attributes of the construction are its function and the geological characteristics of the erection site.

The design of structures with geometry, materials and behavior diverse from a usual building are required frequently. However, several statements are found in the mentioned documents implying that the comprised information is not to be applied in these cases. According to [Sprague and Legatos \(2000\)](#), the building code development process has traditionally given little effort to developing the seismic design process of nonbuilding structures. Nevertheless, they are often the only tool available to predict the seismic behavior of such structures.

This article deals specifically with machines for paper production ([Figure 1](#)), whose resistant system constitutes of moment-resisting steel frames, which support metallic rotors on whose surface the paper web is in contact with. These mechanical equipments comprise independent sections, being the most important: wire section, press section, dryer section and end section. Water is usually removed in three stages: drainage, pressing and heating.

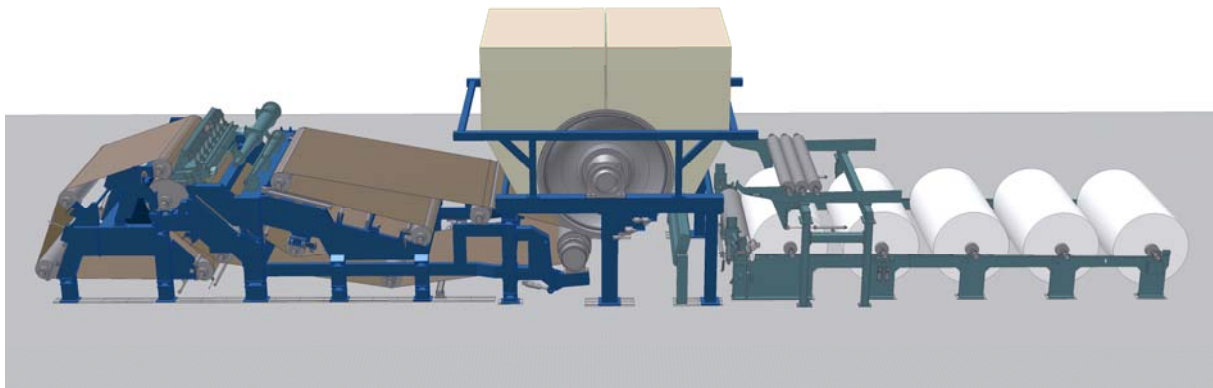


Figure 1: Machine for tissue paper production

Different machines are required for the production of different paper classes. These classes are sorted mostly by base weight, coating, manufacturing process and raw material. This article deals with part of a machine for the production of tissue paper, used for napkins and handkerchiefs, for instance.

A basic plane model was studied ([Figure 2](#) / [Figure 3](#)), calculated analytically and by means of the finite element method (FEM). The understanding of related literature and the most common analysis methods was intended. Significant assumptions were negligible vertical displacements and lumped masses at nodes.

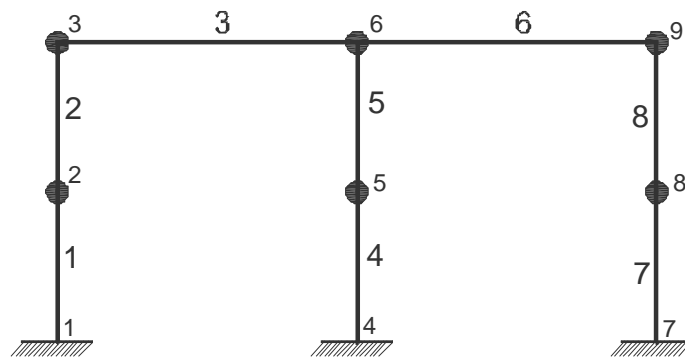


Figure 2: Plane model beams and nodes numbering

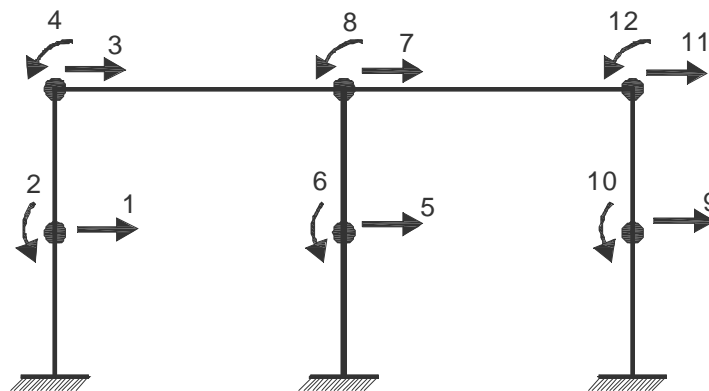


Figure 3: Active degrees of freedom of plane model

## 2 SEISMIC LOADING

As aforementioned, the information in this section and the loading cases considered were based mostly on the Brazilian code for seismic design - [NBR 15421](#), even though additional comments are provided.

The first variable to be defined is the design horizontal acceleration,  $a_g$ , found by means of the seismic zones map (see [Figure 4](#)). The values in this figure are valid for soil classified as rock, or otherwise with shear wave velocity between 760 m/s and 1500 m/s, and should be corrected in case of different soil classes. As a general rule, softer soils amplify the seismic waves and therefore seismic loads.

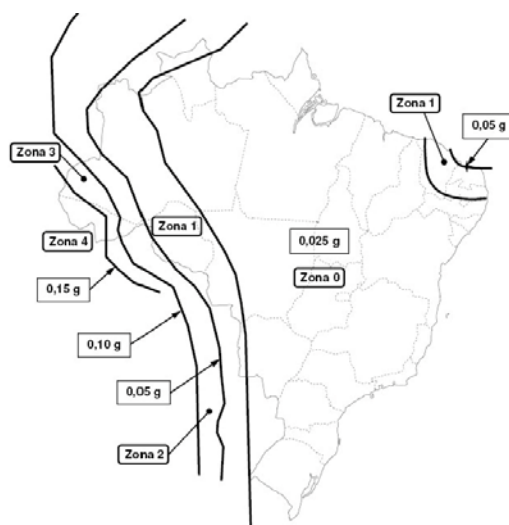


Figure 4: Brazilian seismic zones – Source: NBR 15421

Structures with different dynamic behavior perform in a different way during an earthquake. For that reason, another important concept is the design spectrum, which defines the amplification or even reduction of the horizontal acceleration as a function of the natural period or frequency (see Figure 5). The design horizontal acceleration ( $a_g$ ) corresponds to the amplitude at a period of 0 s, meaning a rigid construction that present the same acceleration from its foundation. Furthermore, spectra are often defined for a damping factor of 5%, though amplitude corrections are permitted if correctly reasoned.

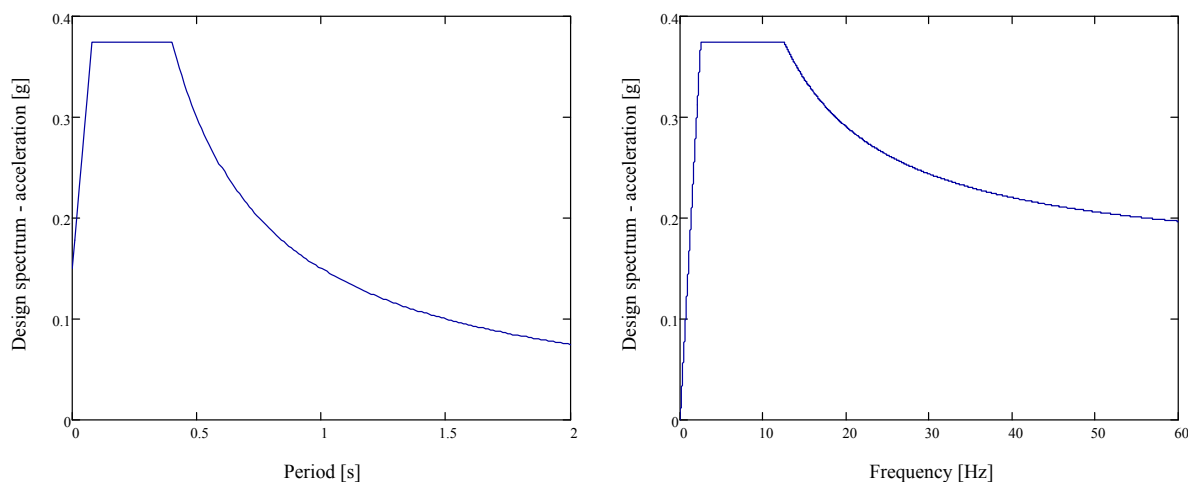


Figure 5: Design spectrum from NBR 15421 –  $S_a(T)$  left /  $S_a(f_n)$  right

In addition, the basic seismic resistant system must be acknowledged. This classification allows the identification of the response modification and displacement amplification coefficients ( $R$  and  $C_d$ , respectively). The first one has the purpose of expressing all the energy dissipation sources, not present in a linear elastic analysis. The latter ( $C_d$ ) has the purpose of correcting the displacements found, also affected by the response modification coefficient ( $R$ ). The studied structure was classified as steel moment resisting frames with ordinary detailing.

The importance coefficient is an additional scale factor applied to the load values, chosen with regard to the construction occupation, and causing amplification according to the

significance of the structure. As an example, a hospital building would receive a higher coefficient than an ordinary warehouse.

Soil type rock and ordinary construction occupation were arbitrarily chosen so importance coefficient and soil amplification (embedded in  $a_g$  value) resulted in unity values.

A summary of the required classifications and resulting coefficients or values are presented in [Table 1](#).

Denomination	Classification	Coefficients / values
Horizontal acceleration ( $a_g$ )	Erection site (zone 4) / Soil Class (Rock)	0,15 g
Design spectrum acceleration ( $S_a$ )	Natural frequencies / periods	<a href="#">Figure 5</a>
Response modification coefficient (R)	Seismic resistant system - Steel moment resisting frame with ordinary detailing	3,5
Displacement amplification coefficient ( $C_d$ )		3
Importance coefficient (I)	Construction occupation (ordinary)	1

Table 1: Required classifications and resulting coefficients or values

## 2.1 Equivalent lateral forces

The equivalent lateral forces method is the simplest one presented, consisting of the application of static forces proportional to gravity loads. It reckons the response in the fundamental mode as predominant, although influence of higher modes is taken into account in some way.

Total base shear is found by equation 1:

$$H = C_s W \quad (1)$$

Where:

$C_s$  – seismic response coefficient

$W$  – system weight

The seismic response coefficient is a function of natural period, comprising the design spectrum amplitude ( $S_a$ ), the response modification (R) and the importance coefficients (I). Although, differences exist between its shape and the one from the previously defined design spectrum (see [Figure 5](#) / [Figure 6](#)), since there is a predefined lower boundary of 0,01 and no reduction for higher frequencies.

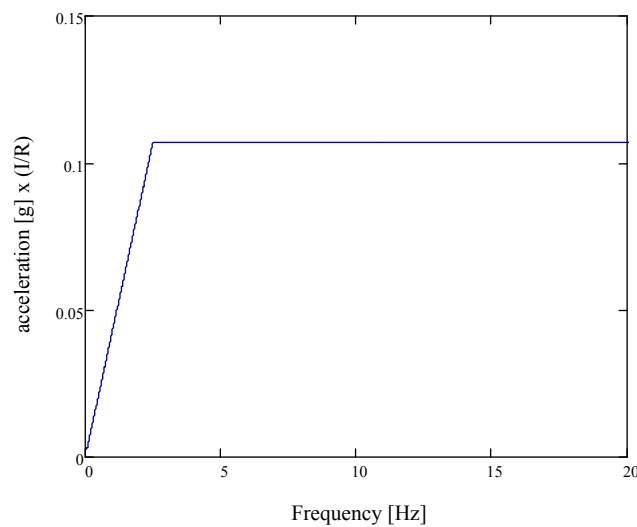


Figure 6: Seismic response coefficient

The influence of higher modes is accounted for by means of a vertical distribution of the total horizontal base shear among several elevations in the structure. It is defined by the vertical distribution coefficient, given by equation 2.

$$C_{vx} = \frac{w_x h_x^k}{\sum_{i=1}^N w_i h_i^k} \quad (2)$$

Where:

$w_x / w_i$  – weight related to elevation  $x / i$

$h_x / h_i$  – value of elevation  $x / i$  with regard to base level

$k$  – distribution exponent, ranging from 1 to 2. As a general rule, it increases with increasing natural periods.

Lastly, the force in a given elevation  $x$  is found by equation 3.

$$F_x = C_{vx} H \quad (3)$$

Nevertheless, the displacements found by application of loads calculated by equation 3 ( $u_0$ ) must be corrected by the displacement amplification ( $C_d$ ) and importance coefficients ( $I$ ) (equation 4).

$$u = \frac{C_d u_0}{I} \quad (4)$$

## 2.2 Spectrum response

The complete response history is seldom needed for structural design, and frequently simply the maximum response is sufficient. As a result, static analyses could be applied for the solution.

This method is based on the superposition principle, and therefore may only be applied to structures with linear behavior. Furthermore, since the phase between the modal contributions is not found, some form of combination is required.

In a simplified way, the contribution of each natural mode comes from the design spectrum. As an example, the acceleration amplitudes corresponding to the first two natural modes are shown in Figure 7. The number of modes considered should be sufficient to hold at least 90% of the total mass as effective masses in each of the orthogonal directions analyzed.

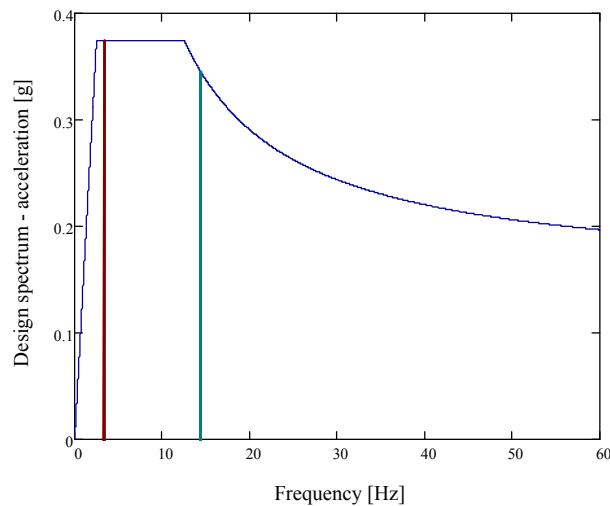


Figure 7: Design spectrum

The direct sum of results would be excessively conservative, given that the occurrence of the maximum values at the same time is quite improbable. The square root of sum of squares method (SRSS), given by equation 5, was applied, where  $e^t$  is the total response and  $e_r$  the contribution of mode  $r$ .

$$e^t = \sqrt{\sum_{r=1}^N e_r^2} \quad (5)$$

### 2.3 Transient – acceleration time history

The transient method employs accelerograms, representative of the seismological characteristics of the erection site, applied to the structure base. At least three sets of accelerograms, mutually independent, should be considered in the analysis. Moreover, the maximum responses among them should be considered.

These accelerograms must be affected by a scaling factor, so that the response spectra in the studied direction present average results not lower than the average value of the design spectrum in a range of  $0,2$  to  $1,5 T$ , where  $T$  is the fundamental period in this direction.

## 3 NATURAL FREQUENCIES AND VIBRATION MODES

The governing equation of motion for a multiple degree of freedom system subjected to an identical ground motion in all supports is given by equation 6. Both the damping and the excitation terms are removed for the determination of natural properties, resulting in equation 7.

$$\mathbf{M}\ddot{\mathbf{u}}(t) + \mathbf{C}\dot{\mathbf{u}}(t) + \mathbf{K}\mathbf{u}(t) = -\mathbf{M}\ddot{\mathbf{u}}_g(t) \quad (6)$$

$$\mathbf{M}\ddot{\mathbf{u}}(t) + \mathbf{K}\mathbf{u}(t) = \mathbf{0} \quad (7)$$

This equation is characteristic of an eigenvalues and eigenvectors problem, whose results are found by means of equations 8 and 9. In addition, the mass matrix normalization was performed to all eigenvectors.

$$\omega_{nr}^2 = \text{eigenvalues}(\mathbf{M}^{-1}\mathbf{K}) \quad (8)$$

$$\phi_r = \text{eigenvectors}(\mathbf{M}^{-1}\mathbf{K}) \quad (9)$$

The results found are presented in Table 2.

Mode	$\omega_{nr}$ [rad/s]	$T_{nr}$ [s]	FEM results
1	21,0	0,2996	Figure 8
2	90,4	0,0695	Figure 9
3	141,7	0,0443	
4	350,3	0,0179	
5	521,4	0,0121	
6	559,6	0,0112	
7	661,9	0,0095	
8	720,8	0,0087	
9	752,2	0,0084	
10	887,1	0,0071	
11	1042,1	0,0060	
12	1301,4	0,0048	

Table 2: Natural frequencies and periods

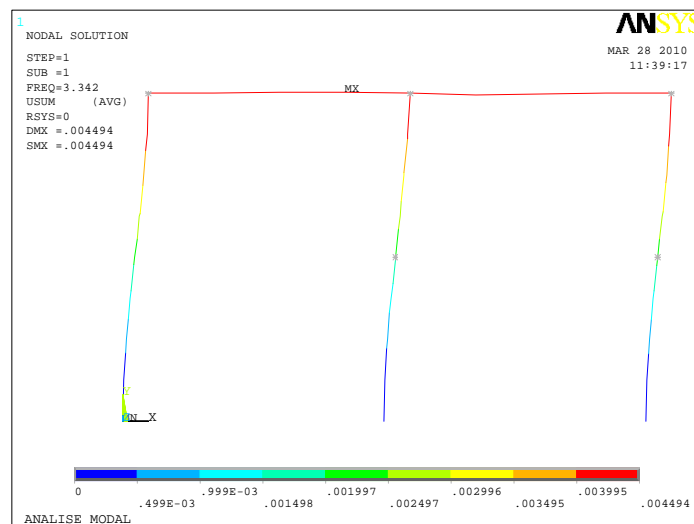


Figure 8: 1<sup>st</sup> vibration mode

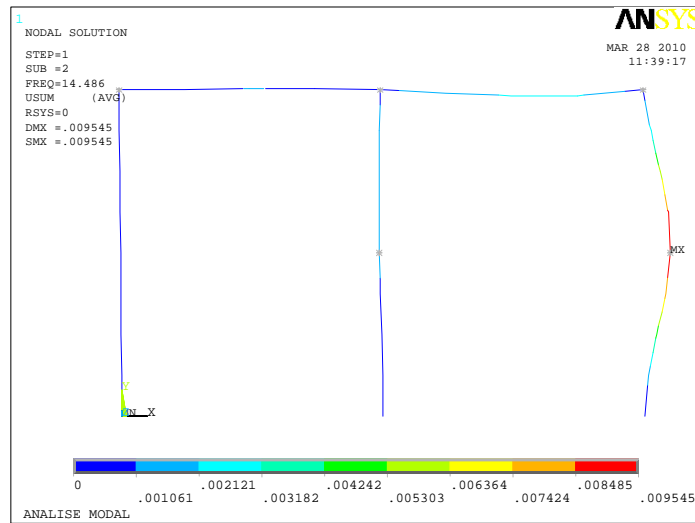


Figure 9: 2<sup>nd</sup> vibration mode

#### 4 EXCITATION VECTOR EXPANSION

The equivalent excitation vector resultant from the base excitation is given by equation 10.

$$\mathbf{p}_{\text{eff}} = -\mathbf{M}\mathbf{t}\ddot{\mathbf{u}}_g(t) \quad (10)$$

The vector  $\mathbf{t}$  describes the direction of seismic loading, by means of unity values in the appropriate positions. The studied load case was a horizontal earthquake; hence  $\mathbf{t}$  is given by equation 11.

$$\mathbf{t}^T = \{1 \ 0 \ 1 \ 0 \ 1 \ 0 \ \dots \} \quad (11)$$

The spatial distribution of the excitation is given by vector  $\mathbf{s}$ , not time dependent, defined by equation 12. The time variation is given by the scalar function  $-\ddot{\mathbf{u}}_g(t)$ . Moreover, it is suitable to expand this vector with regard to the contribution of each natural mode (equation 13).

$$\mathbf{s} = \mathbf{M}\mathbf{t} \quad (12)$$

$$\mathbf{s} = \sum_{r=1}^N \mathbf{s}_r = \sum_{r=1}^N \gamma_r \mathbf{M}\boldsymbol{\phi}_r \quad (13)$$

According to Chopra (2006), the excitation vector expansion has two useful properties: the load vector  $-\mathbf{s}_r\ddot{\mathbf{u}}_g(t)$  produces response in mode  $r$  but no response in any other mode, and response in mode  $r$  is due entirely to this vector. Moreover, the results for certain response ( $\mathbf{e}_r(t)$ ), as displacement or reactions, may be found by equation 14.

$$\mathbf{e}_r(t) = \mathbf{e}_r^{\text{st}} \left[ \omega_{nr}^2 \frac{\mathbf{q}_r(t)}{\gamma_r} \right] \quad (14)$$

Where  $\mathbf{e}_r^{\text{st}}$  is the response due to the static application of vector  $\mathbf{s}_r$ , and  $\mathbf{q}_r(t)$  the modal coordinate of mode  $r$ , found by the solution of equation 15, itself obtained via the mode superposition method. In addition, the modal participation factor ( $\gamma_r$ ) is given by equation 16.

$$\ddot{q}_r(t) + 2\xi_r \omega_{nr} \dot{q}_r(t) + \omega_{nr}^2 q_r(t) = \gamma_r \ddot{u}_g(t) \quad (15)$$

$$\gamma_r = \boldsymbol{\phi}_r^T \mathbf{s} \quad (16)$$

The modal contribution factor is defined as the ratio between  $e_r^{st}$  and  $e^{st}$  (equation 17), where the latter means the resulting value due to the static application of  $\mathbf{s}$ . These factors present the property expressed by equation 18, meaning they can be employed as an estimate of the number of modes required for appropriate results regarding certain response.

$$\bar{e}_r = \frac{e_r^{st}}{e^{st}} \quad (17)$$

$$\sum_{r=1}^N \bar{e}_r = 1 \quad (18)$$

The modal contribution factors for the 12 modes, as well as their sum, for the node 4 shear force and moment reactions are presented in Table 3.

Mode	$\bar{V}^{s_r}$	$\sum_{i=1}^r \bar{V}^{s_i}$	$\bar{M}^{s_r}$	$\sum_{i=1}^r \bar{M}^{s_i}$
1	0,919	0,919	0,961	0,961
2	-0,015	0,904	-0,009	0,952
3	0,094	0,998	0,047	0,999
4	0,001	0,999	0,000	1,000
5	0,000	0,999	0,000	1,000
6	0,000	0,999	0,000	1,000
7	0,001	0,999	0,000	1,000
8	0,000	0,999	0,000	1,000
9	0,000	0,999	0,000	1,000
10	0,000	0,999	0,000	1,000
11	0,000	0,999	0,000	1,000
12	0,001	1,000	0,000	1,000

Table 3: Modal contribution factors

## 5 EFFECTIVE MASSES

According to Clough and Penzien (2003), the effective masses are calculated by equation 19. Moreover, one can prove that the sum of effective masses for all modes is equal to the total mass of the system (equation 20).

$$M_r^* = \gamma_r^2 \quad (19)$$

$$M_t = \sum_{r=1}^N M_r^* \quad (20)$$

A physical interpretation of the effective masses is the value that times the spectral acceleration for mode  $r$ , results in the total base shear related to the contribution of this mode

(equation 21).

$$V_{or} = M_r^* S_{ar} \quad (21)$$

The modal participation factors, as well as the effective masses for the 12 modes are presented in Table 4.

Mode	$\gamma_r$	$M_r^* \text{ [kg]}$
1	-246,6	60793,3
2	43,9	1930,6
3	60,7	3686,6
4	-11,1	124,2
5	2,2	4,7
6	-1,6	2,6
7	-5,8	33,8
8	0,0	0,0
9	-2,6	7,0
10	3,3	10,7
11	-4,0	15,7
12	-5,4	29,5

Table 4: Modal participation factors and effective masses

## 6 SEISMIC ANALYSES

### 6.1 Equivalent lateral forces

The loads distribution was determined according to equation 3, with a distribution exponent (k) equal to unity.

The displacements were calculated by equation 22, and the reactions by equation 6, although considering the restrained degrees of freedom as well.

$$\mathbf{X} = \mathbf{K}^{-1}\mathbf{F} \quad (22)$$

The displacements found must be corrected according to equation 4.

### 6.2 Spectrum response

The displacements due to mode r were calculated by equation 23, and the total displacements and reactions found by SRSS combination.

$$\mathbf{u}_r = \gamma_r \frac{S_{ar}}{\omega_{nr}^2} \phi \quad (23)$$

It is worth to mention that reactions could be found by means of the  $\mathbf{u}_r$  results and the stiffness matrix prior to combination operations only, since signs are lost afterwards due to squaring operations.

The displacements found via the FEM model for the 1<sup>st</sup> and 2<sup>nd</sup> mode, as well as the total response, are presented in figures 10 to 12.

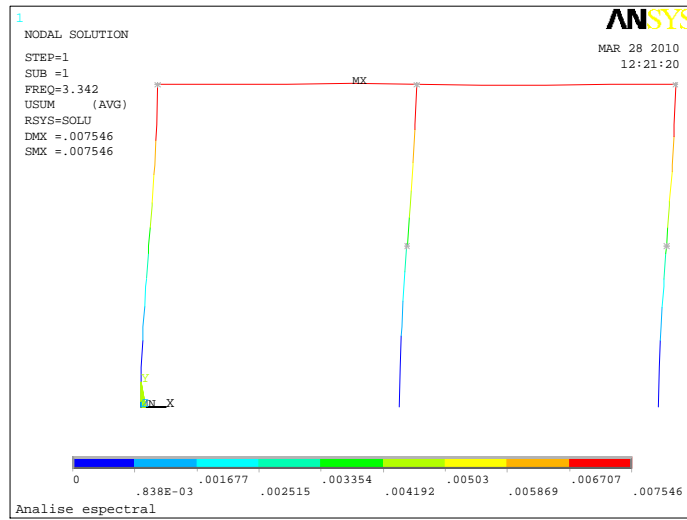


Figure 10: 1<sup>st</sup> mode displacements

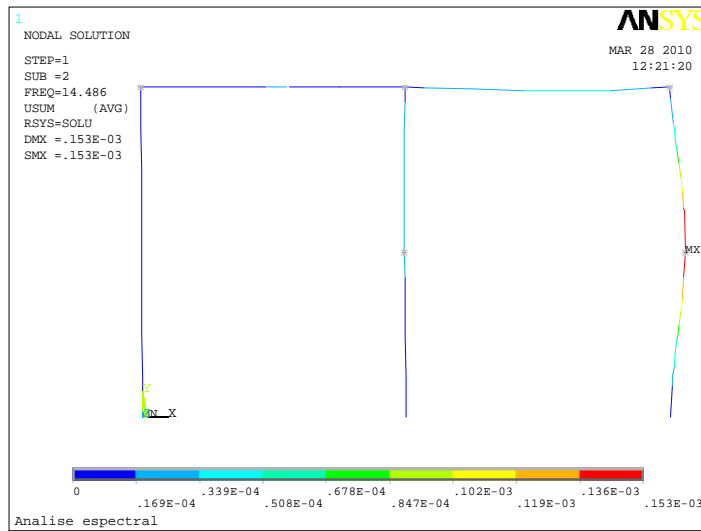


Figure 11: 2<sup>nd</sup> mode displacements

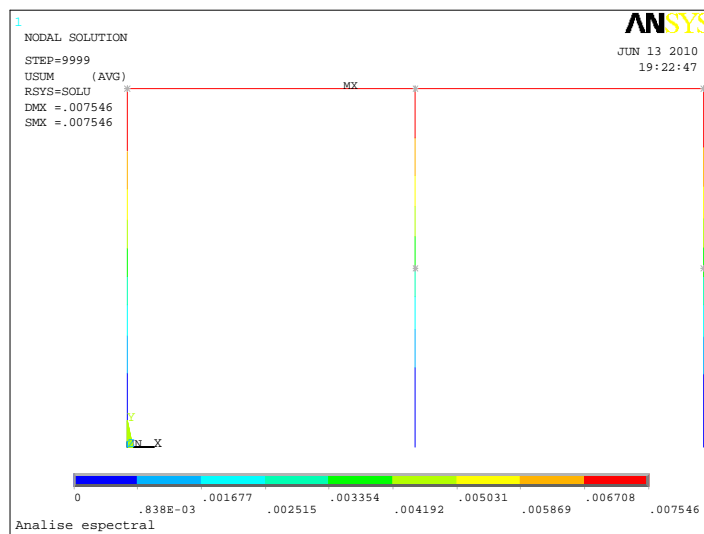


Figure 12: Total displacements

### 6.3 Transient with acceleration time history

The displacements were found by equations 24 and 25, based on the modal superposition method. The uncoupled equations of motion are given by equation 15.

$$\mathbf{u}(t) = \sum_{r=1}^N \mathbf{u}_r(t) \tag{24}$$

$$\mathbf{u}_r(t) = \phi_r \mathbf{q}_r(t) \tag{25}$$

The accelerograms selection criteria must be chosen carefully, with regard to event magnitude and soil type. All data were obtained from COSMOS, and next scaled as described in 2.3.

The selection criteria chosen were magnitude of the seismic event  $7 \pm 0,2$  in Richter scale and soil type rock. Furthermore, the maximum values found from the independent applications of three accelerograms were considered.

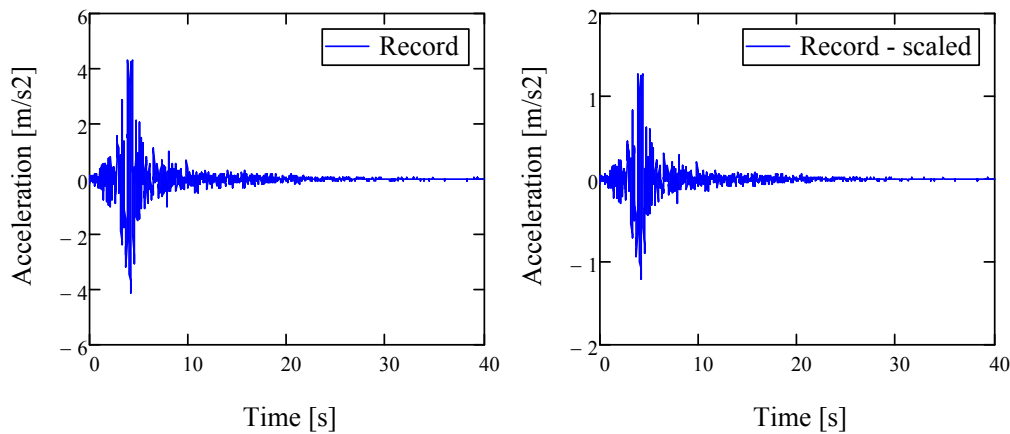


Figure 13: Accelerogram 1 – prior to (left) and after scaling (right)

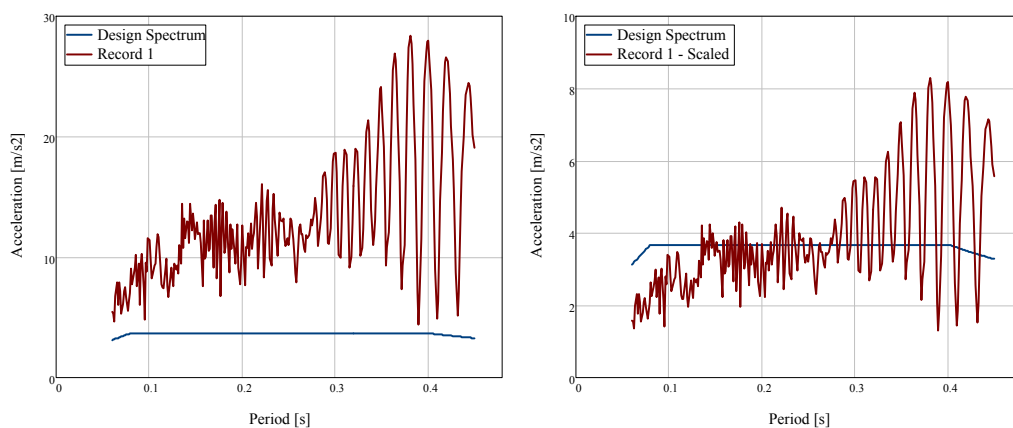


Figure 14: Design spectrum and response spectrum for record 1 – prior to (left) and after scaling (right)

The results found for displacements of node 6 and reactions at node 4, due to application of accelerogram 1, are presented in figures 15 to 17.

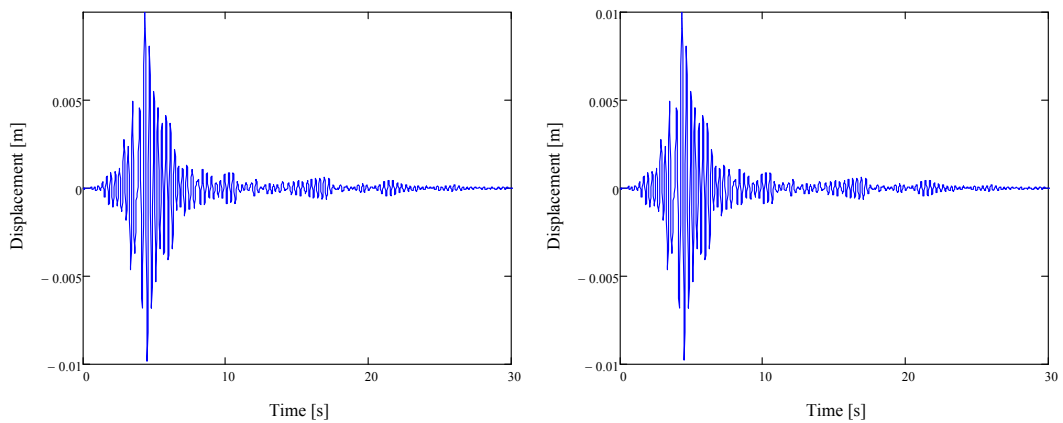


Figure 15: Displacement of node 6 – 1<sup>st</sup> mode (left) and total (right)

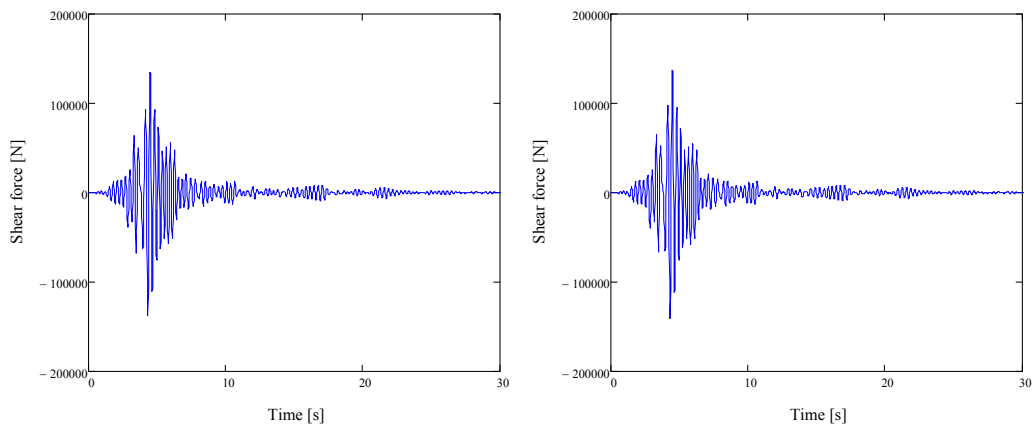


Figure 16: Shear force reaction at node 4 – 1<sup>st</sup> mode (left) and total (right)

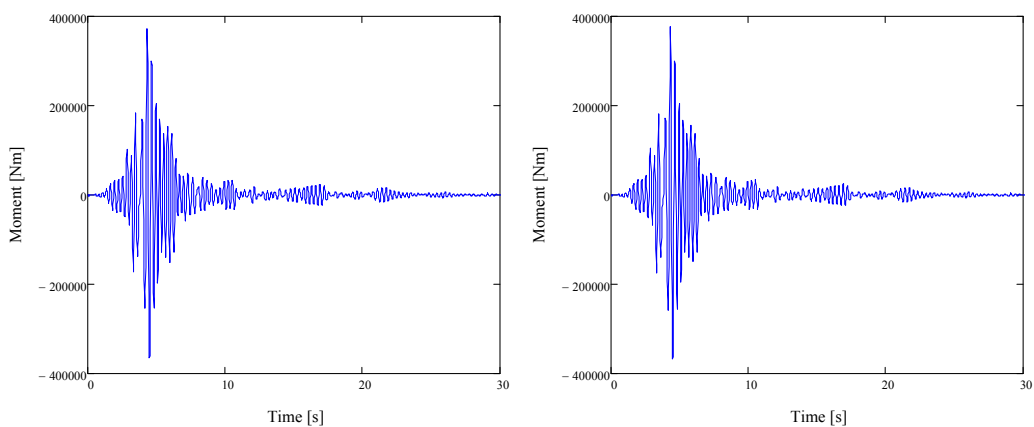


Figure 17: Moment reaction at node 4 – 1<sup>st</sup> mode (left) and total (right)

## 7 CONCLUSIONS

The results were assessed in Table 5, more specifically by means of the ratios between the values found for each method and those for the spectrum response analysis with FEM, presented in the last column on the right. This comparison method was chosen arbitrarily in order to make results examination easier.

Result	Analytical methods						FEM
	Equivalent Lateral Force				Spectrum (SRSS)	Transient	Spectrum (SRSS)
	k=0	k=1	k=2	k=3			
Shear force node 1	-1,003	-1,084	-1,138	-1,170	0,998	1,405	1,000
Moment node 1	1,000	1,085	1,142	1,175	0,999	1,408	1,000
Shear force node 4	-1,081	-1,092	-1,099	-1,103	0,998	1,397	1,000
Moment node 4	1,039	1,090	1,124	1,144	1,000	1,405	1,000
Shear force node 7	-1,148	-1,080	-1,036	-1,009	0,998	1,416	1,000
Moment node 7	1,081	1,086	1,089	1,091	0,999	1,417	1,000

Table 5: Assessment of results for all methods – ratio with regard to FEM spectrum analysis with SRSS

Most results found with the transient analysis were higher. However, this was attributed to problems regarding the criteria applied for the input accelerograms selection, since an excessive deviation was found even between the results from the three records (Table 6).

Result	Transient			
	Accel. 1	Accel. 2	Accel. 3	Maximum
Shear force node 1	0.919	0.711	1.000	1.000
Moment node 1	0.940	0.711	1.000	1.000
Shear force node 4	0.939	0.720	1.000	1.000
Moment node 4	0.954	0.715	1.000	1.000
Shear force node 7	0.944	0.719	1.000	1.000
Moment node 7	0.950	0.714	1.000	1.000

Table 6: Assessment of transient analysis results – ratio with regard to maximum values

Even though the transient analysis is the most accurate, its results were not satisfactory, since problems with input data were noticed. The selection criteria should be revised prior to trying this method, since computational effort is extremely high when compared to others.

The equivalent lateral force method presented higher values as well; nonetheless the maximum deviation found with a distribution exponent equal to unity, indicated by the followed building code for the studied period range, was 9% on the safe side. Since this is a much simpler analysis, it could be applied with the motivation of less computational and engineering time and effort.

It is worth to restate that the model considered was extremely simplified; and its most important purpose was the understanding of related literature. Therefore, the conclusions above should be taken with caution for actual equipments. A next step would be to assess the results of these analyses for more accurate tridimensional models.

## REFERENCES

Associação Brasileira de Normas Técnicas, *NBR 15421: Projeto de estruturas resistentes a sismos – procedimento*. 2006.

- Chopra, A.K., *Dynamics of structures: Theory and applications to earthquake engineering*, 3<sup>rd</sup> ed. Prentice Hall, 2006.
- Clough, R.W., Penzien, J., *Dynamics of structures*, 3<sup>rd</sup> ed. Computers & Structures, 2003.
- Consortium of Organizations for Strong-Motion Observation Systems (COSMOS), COSMOS Virtual Data Center. Web-site: <http://db.cosmos-eq.org/>, 2010.
- Sprague, H.O., and Legatos, N.A., Nonbuilding structures seismic design code developments. *Earthquake Spectra*, 16:127-140, 2000.